NEUTRON DIFFRACTION ANALYSIS OF CYTOCHROME b_5 RECONSTITUTED IN DEUTERATED LIPID MULTILAYERS

E. P. GOGOL AND D. M. ENGELMAN
Department of Molecular Biophysics and Biochemistry, Yale University, New Haven, Connecticut 06511

G. ZACCAI
Institut Laue-Langevin, 38042 Grenoble, France

ABSTRACT Cytochrome b_5 was reconstituted with a highly deuterated phospholipid to form ordered multilayers consisting of repeated centrosymmetric pairs of asymmetric lipid-protein bilayers. Lamellar neutron diffraction data were collected to ~29 Å resolution, and have been interpreted using models for the interaction of the membrane-binding domain of cytochrome b_5 with the lipid bilayer. A range of different models was examined, and those in which the protein penetrates well into the bilayer, possibly spanning it, are favored.

INTRODUCTION

Membrane proteins that have hydrophobic interactions with a lipid bilayer can be divided into two classes: globular and anchored. Globular membrane proteins have substantial tertiary structure within the hydrophobic region of the lipid bilayer, and appear to be necessary for transport across membranes. Another class of hydrophobically bound membrane proteins, including certain enzymes and cell surface proteins, has no obvious requirement for a transmembrane structure. Transmembrane sequences have nevertheless been identified in a number of these anchored proteins, primarily by chemical modification; however, the methodologies used do not permit the identification of anchored proteins that do not span the membrane. Hence, no universal model for anchored membrane proteins has yet emerged.

Cytochrome b_5 is an example of an anchored protein whose function, electron transfer between other membrane proteins, does not appear to require a membrane-spanning sequence. It is an amphipathic protein of the endoplasmic reticulum, and is proteolytically separable into two domains, a catalytic heme-containing fragment and a carboxyl-terminal, membrane-binding peptide (Spatz and Strittmatter, 1971). While both domains have been well-characterized biochemically and structurally (see reviews by Hagihara et al., 1975, and von Jagow and Sebald, 1980), the distribution of the hydrophobic domain within the membrane has not been elucidated. Energy transfer measurements have localized a particular tryptophan residue in the hydrophobic domain near the center of the bilayer (Fleming et al., 1979), and chemical reactivity measurements indicate that the carboxyl and amino termini are located on the same side of the membrane (Dailey and Strittmatter, 1981). Based on these and other data, a folding scheme and membrane location for the hydrophobic peptide have been proposed (Fleming et al., 1978; Dailey and Strittmatter, 1981) in which the tail is folded into a small domain, located near the center of the bilayer. Other tertiary arrangements may be consistent with the pertinent observations, however, including structures that would penetrate the bilayer to various depths.

X-ray diffraction studies of native and reconstituted one-dimensionally ordered membranes have contributed to the understanding of their architecture (e.g., Wilkins et al., 1971; Dupont et al., 1973; Kirshner et al., 1975; Yeager et al., 1980; Herbette et al., 1981). With the exception of the purple membrane of *Halobacterium halobium* (Blaurock, 1975), interpretation in terms of molecular structure has been limited by several factors: the resolution of the data, the low natural contrast between lipid and protein, the heterogeneity of proteins in most natural membranes, and the lack of auxilliary structural knowledge of the protein examined. A neutron diffraction analysis of cytochrome b_5, incorporated into ordered lipid multilayers, promised to overcome several of these limitations. The use of neutrons rather than x-rays has several advantages for the examination of membrane structures (Schoenborn, 1976; Zaccai, 1978), in particular, the greater relative contrast between membrane components. In addition, the large difference between the scattering lengths of the stable isotopes of hydrogen can be exploited both by H_2O-D_2O exchange and by selective deuteration of part of the structure.

Dr. Gogol's current address is Department of Structural Biology, Stanford University School of Medicine, Stanford, CA.

EXPERIMENTAL METHODS

Materials

Steer liver cytochrome b_5 was prepared by Dr. Phillip Strittmatter as previously described (Strittmatter et al., 1978). Protein concentration was routinely determined using a molar extinction coefficient of 117,000 at 413 nm (Spatz and Strittmatter, 1971).

Lipids were extracted according to Bligh and Dyer (1959) from 100–250 g of cell wall and membrane pellets isolated from *E. coli* MRE600, which had been grown in minimal medium dissolved in 100% D_2O (Moore et al., 1975). Phosphatidylethanolamine was isolated by silicic acid chromatography, and converted to phosphatidylcholine (PC) by methylation (Stockton et al., 1974) with deutero-iodomethane (Merck Chemical Div., Merk & Co., Rahway, NJ). Fractions containing pure PC were pooled, concentrated, and stored under nitrogen at −20°C. Lipid identity and purity (at least 98% in the final product) were assessed by thin-layer chromatography (TLC), and lipid concentrations were determined by dry weight and phosphate assay (Bartlett, 1959), which together gave an average PC molecular weight of 810 ± 40. Fatty acid composition was analyzed by gas chromatography of the methyl esters of the free fatty acids (Morrison and Smith, 1964). The fatty acids included saturated, unsaturated, and branched chains 14–20 carbons long (average length 16.5 carbons), and the overall composition was not significantly altered by methylation.

The deuteration level of the lipid was determined by proton NMR performed with the 270 MHz Bruker spectrometer (Bruker Instruments, Inc., Billerica, MA) at the New England High Field NMR Facility, New Haven, CT. Proton resonances were assigned by comparison with a published PC spectrum (Chapman and Morrison, 1966), and integrated peak areas from parallel deuterated and nondeuterated samples were compared, using the fully H-exchanged amino hydrogens as an internal standard. The average deuteration level thus measured was 91% for the acyl chains, and 80% for the glycerophosphorylcholine group (including 100% deutero-methyls on the choline moiety).

Sample Preparation

Ordered lipid and lipid-protein multilayers were formed from sonicated vesicles. Vesicles were prepared by the method of Huang (1969): 5–10 ml of buffer (20 mM Tris-acetate, pH 8.1, 0.2 mM EDTA, 0.02% NaN_3) was added to 50–100 mg of dry lipid, and the mixture was sonicated for 2 h at 0°C. The suspension was centrifuged at 100,000 *g* for 30 min, and the supernatant, containing 60–90% of the lipid, was stored under nitrogen at 0°–4°C for up to 4 d. TLC analysis indicated <2% breakdown of the lipid under these conditions. Cytochrome b_5 was incorporated into preformed vesicles in a "tight binding" mode (Enoch et al., 1979) by sonicating a mixture of vesicles and protein for 2 h at 20°–30°C. Binding was assayed by gel filtration on Sepharose 4B (Pharmacia Fine Chemicals, Div. of Pharmacia Inc., Piscataway, NJ). The asymmetry of protein distribution across the vesicle bilayer (>95%) was determined by measuring the extent of reduction of cytochrome b_5 with NADH and externally added cytochrome b_5 reductase soluble fragment, before and after disruption of the vesicles (Rogers and Strittmatter, 1975). Vesicles used for multilayer preparation were dialyzed against 2 mM Tris-acetate, pH 8.1, to lower the ionic strength to prevent crystallization of buffers on dehydration. Suspensions containing 2–10 mg of lipid were spread on acid-washed glass microscope slides and partially dried at 38°C under a gentle stream of humidified nitrogen (maintained at 75% relative humidity for lipid-protein multilayers). The visible absorption spectrum of cytochrome b_5–lipid multilayers showed no significant difference from that of the free or vesicle-bound protein.

Diffraction Experiments

Lameller diffraction patterns were collected using a neutron diffractometer, instrument D16 at the Institut Laue Langevin. The instrument was operated as described by Buldt et al. (1979), except that horizontal collimation was achieved by use of vertical Soller slits in the incident and diffracted beams, giving a resolution in 2θ of 0.7° and 0.2° for the lipid and cytochrome b_5–lipid multilayer experiments, respectively. The beam dimensions were reduced to 1 cm × 1 cm by B_4C-impregnated masks placed in front of and behind the sample. Samples were equilibrated with argon that had been partially humidified by bubbling through saturated salt solutions made up with various H_2O-D_2O mixtures. Bragg reflections were measured using ω-2θ scans, and exposure times were controlled by a beam monitor; the weaker higher-order reflections were collected for longer times and scaled to constant monitor counts.

The mosaic spreads of the samples were measured with ω-scans, in which the detector was held at a diffracting position and the sample was rotated in the incident beam. For all data reported here, the mosaic spreads were ~1° or less (full width at half maximum), and were often less than the angular resolution of the diffractometer. Sample attentuations were determined by scanning the direct beam transmitted through the sample held in a series of orientations.

Data Treatment

Smooth background curves, estimated from the small-angle scatter and the minima between reflections, were subtracted from the data. Diffraction intensities $I(h)$ were measured for each reflection by summing the resulting points in each peak. Error estimates were obtained from the statistical errors in the data points and the variability in potential background curves.

Structure factors $F(h)$, where h is the diffraction order, were derived from integrated intensities, $I(h)$, after correcting for systematic errors (Buldt et al., 1979):

$$F(h)^2 = I(h) \cdot L(h) \cdot V(h) \cdot P(h) \cdot A(h). \qquad (1)$$

The Lorentz factor, $L(h)$, is equal to sin 2θ for ω-2θ diffraction geometry, and is approximated by h at the small angles used. $V(h)$ is a correction that takes into account the limited vertical acceptance of the detector (Saxena and Schoenborn, 1977). A geometrical calculation indicated that no correction is needed for the angular ranges examined; this was confirmed by taking data with a reduced detector acceptance, and finding no alteration in the ratios of intensities of different peaks. $P(h)$ is a correction applied only when the projection of the sample normal to the beam is larger than the illuminating beam; a simple geometrical factor was applied for data taken with $\omega > 9.6°$ (lipid multilayers only). The angular dependence of attentuation by the sample is corrected for by $A(h)$, which can be calculated for a thin planar sample (Worcester and Franks, 1976), or estimated from sample transmissions.

Structure factors measured at various H_2O-D_2O ratios (from a single sample at constant relative humidity) were plotted vs. solvent-scattering density. Error-weighted linear regressions to these points generally gave correlation coefficients of 0.99, and allowed improved estimates of the structure factors to be made. In the case of very strong reflections, in particular the first order of lipid multilayers and the second order of cytochrome b_5–lipid multilayers, primary extinction effects were detected and corrected (Fig. 1 *B*) (Caspar and Phillips, 1975; Worcester and Franks, 1976). A correction of 20% was applied to a single structure factor in the worst case. One reflection, the first order of protein-lipid samples, was difficult to measure at high D_2O contents due to the relatively strong small-angle scattering present. That structure factor was obtained by extrapolating a contrast variation plot from lower solvent D_2O-H_2O ratios (Fig. 1 *A*).

CALCULATIONS AND RESULTS

Deuterated Lipid Profile

An understanding of the neutron-scattering density profile of the deuterated lipid bilayer is prerequisite to interpreting the cytochrome b_5-lipid multilayer diffraction data. To

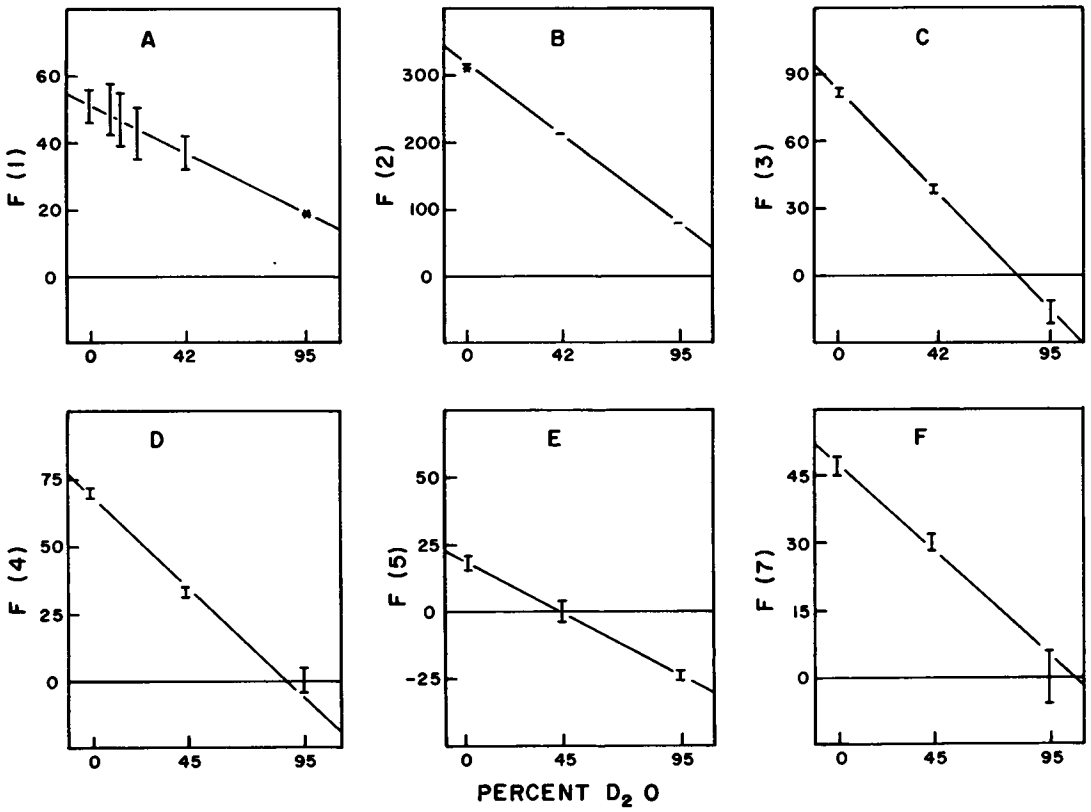

FIGURE 1 Contrast-variation plots of the cytochrome b_5–lipid multilayer data. *A–E*, first through fifth diffraction orders; *F*, seventh order (the sixth order is zero in all H_2O–D_2O mixtures). Structure factors are plotted on a relative scale, and the fraction of D_2O in the water is used as a linear measure of solvent scattering density. Measurement of a weak reflection obscured by strong small-angle scatter in 95% D_2O is shown in *A*, and correction for apparent primary extinction is illustrated in *B* (observed value in H_2O is indicated by the asterisk).

this end, diffraction patterns were collected from lipid multilayers in a series of hydrations and H_2O-D_2O mixtures, and structure factors were derived to ~8 Å resolution (six diffraction orders at a lattice spacing of ~50 Å). The centrosymmetric profile is given by the Fourier summation:

$$\rho(x) = (2/d)\sum_{h=1}^{h_{max}} F(h) \cdot \epsilon(h) \cdot \cos(2\pi hx/d), \qquad (2)$$

where $\rho(x)$ is the one-dimensional projection of scattering length density, d is the lamellar spacing, and the phase dependence $\epsilon(h)$ is limited to values of $+1$ and -1. Phase assignments were arrived at by the convergence of three methods: isomorphous replacement, lattice variation, and model building. H_2O-D_2O exchange in the water layer was used as an isomoprhous replacement site (Zaccai et al., 1975); the water profile was modelled as a Gaussian distribution with a width consistent with difference Patterson analysis. The continuous transform of the bilayer profile was traced by varying the lattice spacing through humidity changes (e.g., Worcester, 1975). The limitations of the data still left uncertainties in the weakest reflections; however, these structure factors made no significant difference in the reconstructed profile.

To obtain a lipid-bilayer profile useful for interpreting the protein structure, an absolute density scale and its solvent dependence was derived by model building. The average anhydrous scattering densities of lipid polar groups and acyl chains were calculated from the scattering lengths of the constituent atoms and the lipid partial molecular volumes (Tardieu et al., 1973); the hydration of the polar region was estimated as 25% by volume, based on its cross-sectional area (Levine and Wilkins, 1971), its volume, and its length in projection (Buldt et al., 1979). The resulting average densities (for a nondeuterated lipid) provide an absolute scale for the neutron profile of egg lecithin (Worcester, 1975), which is in good agreement with other treatments of similar bilayer profiles (e.g., Franks and Lieb, 1979). The egg lecithin profile was divided into 11 pairs of 2-Å-wide strips of density; each was scaled to account for the observed levels of deuteration, and the model was Fourier transformed to predict structure factors by

$$F_{calc}(h) = 4\sum_{n=1}^{11} [\rho(n) - \rho_{solv}] \cdot \frac{\sin(2\pi h)}{2\pi h} \cdot \cos[2\pi hx(n)/d], \qquad (3)$$

where $[\rho(n) - \rho_{solv}]$ is the density difference between the nth strip and solvent, $x(n)$ is the nth strip's position, and the summation is taken over half of the centrosymmetric profile (Worthington, 1969). Phases calculated by this transformation agree with those obtained as described above, and the residual between calculated and observed structure factors, calculated by

$$R = \sum_{h=1}^{h_{max}} |[F_{calc}(h) - F_{obs}(h)]| \sum_{h=1}^{h_{max}} F_{obs}(h) \quad (4)$$

was found to be <0.2 in any H_2O-D_2O mixture. Small and reasonable refinements in the density levels and water distribution (average change of 6% per strip) allow a better match to the observed profile (Fig. 2), giving residuals of 0.04 in H_2O and 0.15 in D_2O (where the relative error in intensity measurement is greater). Based on this agreement, the lipid profile is sufficiently established for use in model building.

Structural Analysis of the Cytrochrome b_5–Lipid Multilayers

Diffraction patterns were collected from several samples prepared from various amounts of material and with a range of lipid-to-protein ratios; observed lattice dimensions and the resolution of the data sets varied. The most successful sample consisted of ~4 mg of vesicles with a molar-lipid-to-protein ratio of 19:1. It had a lattice dimension of 200 Å and gave a pattern consisting of seven reflections, for a resolution of ~29 Å. This data set was collected in three water mixtures, 0, 42, and 95% D_2O, for the minimum information necessary to determine phases changes with solvent contrast (Fig. 1 and Table I). In general, data sets collected from other samples gave lower resolution, split diffraction peaks, or problematic ω-scans, suggesting potential systematic errors.

A preliminary examination of the data, together with consideration of the method of sample preparation, reveals the probable arrangement of the unit cell contents. The observed lattice dimensions are large enough to accomodate two bilayers, together with the corresponding protein and water layers. Formation of the multilayers presumably occurs by collapse and fusion of the asymmetric vesicles, resulting in centrosymmetric pairs of asymmetric bilayers. The linearity of contrast variation plots is consistent with a centrosymmetric unit cell, and a substantial degree of asymmetry in each structure is indicated by the relatively strong odd-numbered reflections.

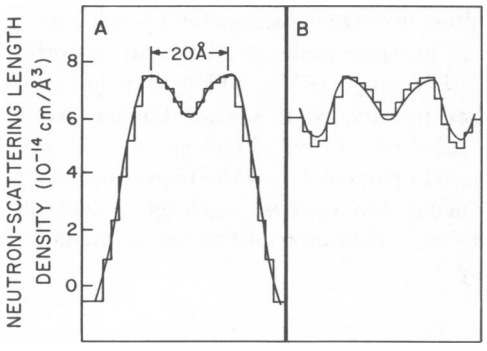

FIGURE 2 Deuterated phosphatidylcholine bilayer profile in H_2O (*A*) and in 95% D_2O (*B*). The reconstructed profiles are designated by the smooth dashed curves, and the density-strip model, on an absolute scale, is represented by the solid step function.

TABLE I
NEUTRON STRUCTURE FACTORS AND PHASES FOR CYTOCHROME b_5–LIPID MULTILAYERS

h	$E(h, H_2O)$*	$F(h, H_2O)$	$F(h, 42\%D_2O)$		$F(h, 95\%D_2O)$
1	+1	51 ± 5‡	37 ± 5		19 ± 10
2	−1	318 ± 1	212 ± 1		78 ± 2
3	+1	82 ± 2	39 ± 2	Δ§	16 ± 5
4	+1	69 ± 2	36 ± 2	Δ	7 ± 5
5	−1	18 ± 3	0 ± 4	Δ	24 ± 2
6	0	0 ± 5	0 ± 5		0 ± 5
7	−1	48 ± 2	29 ± 2		5 ± 6

*Phases listed are derived from model calculations described in the text. They are common to all models with optimized parameters (Table III) except model A1, for which the third and seventh order phase choices are reversed.
‡Errors indicated are estimates of one standard deviation.
§Changes in phase between different H_2O-D_2O mixtures are indicated by Δ.

The Patterson function calculated at each solvent density by

$$P(x) = \sum_{h=1}^{h_{max}} F(h)^2 \cos(2\pi hx/d) \quad (5)$$

contains two peaks of density, centered at 0 and 100 Å, which decrease in size with D_2O content. These features suggest that two deuterated lipid bilayers are present in the unit cell at symmetrical positions. If the unit cell contents are approximated by two Gaussian functions of equal size, their model widths (full width at half maximum), as deduced from the extent of the origin peak, are ~40 Å each, roughly equivalent to the lipid-bilayer dimensions. The difference Patterson function, calculated as above but substituting the difference between structure factors at two solvent densities (taking into account phase changes), represents the self-convolution of the water distribution, along with a smaller contribution from the protein-exchangeable hydrogens. This function contains two peaks separated by 100 Å. The difference in the peak heights and widths indicates that two different water spaces are present in the unit cell. Further direct structural interpretation of the data, by phasing and reconstruction of the profile, proved difficult. The presence of two nonequivalent water spaces complicates phasing, either by H_2O-D_2O exchange or by lattice-dimension variation. Moreover, a low-resolution profile would not be likely to reveal any details of lipid and protein distribution without auxilliary information.

Model Building the Lipid-Protein Profile

Model building offers a way of interpreting the multilayer data that circumvents the problems mentioned above. Termination errors, which distort the profile, are avoided, as are the requirements for phase determination, though phase information directly derived from the data can be included in testing models. Previous structural knowledge of cytochrome b_5 is combined with information from Patterson analysis in the construction of model profiles.

Models were derived by arranging cytochrome b_5 molecules and a lipid bilayer within an asymmetric half-unit cell (half of the centrosymmetric repeat unit) and calculating the resulting projection of neutron scattering density. The dimensions and density profile of the deuterated lipid bilayer were obtained as described above (Fig. 1). Previously determined features of the cytochrome b_5 structure were used to model the protein distribution. The crystal structure of the catalytic segment defines its size and shape as an approximate ellipsoid of 25 Å × 25 Å × 35 Å (Mathews et al., 1971). Hydrodynamic measurements of cytochrome b_5 in detergent solution indicate the presence of an extended, possibly flexible link between protein domains (Visser et al., 1975); two sites accessible to catalytic cleavage (Kajihara and Hagikara, 1968; Ozols and Strittmatter, 1969) suggest the identity of a link region (residues 91–97). The remaining carboxy-terminal sequence (residues 98–133) was assigned to the membrane binding domain, and its volume was calculated from amino acid partial specific volumes. Its distribution was based on the model of bilayer interaction being examined, which determined its partitioning among various regions of the profile (schematically illustrated in Fig. 3 *A*). The average scattering density of each protein segment was calculated (Jacrot, 1976) from its amino acid composition (Ozols and Strittmatter, 1969; Fleming et al., 1978), and by estimating the degree of exchange of labile hydrogens as 80% for the catalytic fragment and linking regions, and 60% for the membrane binding domain.

Several parameters crucial to profile calculation remained indeterminate, and separate profiles were calculated for a range of values for each of these dimensions. Patterson analysis indicated that the bilayers are 100 Å apart, but the limited resolution of the data introduces considerable uncertainty in this figure. A range of bilayer separation distances were explored to optimize the profile for each model. While the catalytic fragment's dimensions are known, its orientation with respect to the bilayer is not; the projection was varied between the possible minimum and maximum values. Finally, the existence and length of the interdomain link is unknown in menbrane-bound cytochrome b_5, and its profile length was varied from 0 Å to a reasonable maximum estimate of 10 Å.

For purposes of Fourier transformation, the 100-Å, half-unit cell was divided into 2-Å strips. The volume fractions of protein, deuterated lipid, and water were calculated for each strip, and its density $\rho(n)$ was determined from the volume-weighted average of the neutron scattering densities. A representative profile is shown in Fig. 3 *B*. Calculated structure factors and phases were derived from the densities and positions of the model profile strips by using Eq. 3.

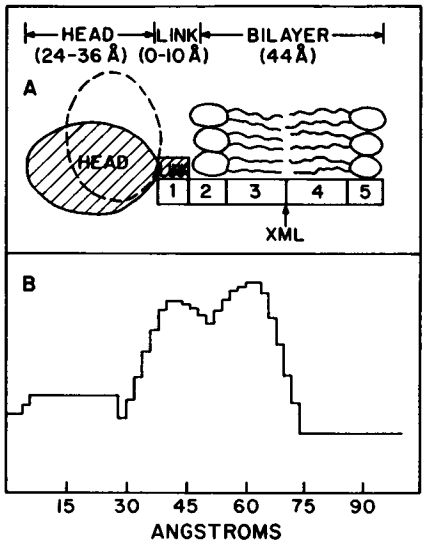

FIGURE 3 (*A*) Parameters used in building the model cytochrome b_5–lipid bilayer profiles. The protein hydrophilic group is depicted as an ellipisoid whose profile projection (*HEAD*) is allowed to vary between 24 and 36 A, and the putative linking region between the protein domains (*LINK*) is varied from 0 to 10 A. The position of the structure in the unit cell is determined by the value of *XML*, which is optimized for the best fit of each model to the data. The protein membrane–binding domain is partitioned among five regions of the profile, which represent the exterior of the bilayer (*1*), the proximal and distal lipid polar (*2* and *5*), and the hydrophobic (*3* and *4*) regions, whose projection lengths are 8 and 14 Å long, respectively. (*B*) The resulting calculated profile for model B1 (half-bilayer protein distribution) with model parameters: head = 28, link = 0, and *XML* = 52.

Comparision of Models

A large number of models for the cytochrome b_5 hydrophobic domain can be constructed and examined within the framework described above. However, the low resolution of the data predicts that discrimination between similar models will be limited. Three significantly different classes of models were chosen to represent possible modes of interaction of protein with the lipid bilayer: A, surface and polar head-group interaction; B, interaction with a single monolayer of lipid; and C, penetration into both halves of the bilayer. The simplest representation of each class of models is an even distribution of the hydrophobic domain, either outside the bilayer (A1) or through one half (B1) or all (C1) of the bilayer. The mass distributions of these models are given in terms of the parameters of Fig. 3 in Table II.

Variations of these general models were also constructed and tested. A mode of lipid-protein interaction proposed for some membrane proteins, though not specifically for

TABLE II
CYTOCHROME b_5 MODEL PARAMETERS: MASS DISTRIBUTIONS OF THE CYTOCHROME b_5 HYDROPHOBIC SEGMENT IN THE MULTILAYER PROFILE

Model	Description	Profile region*				
		1	2	3	4	5
A1	Surface-associated	1.0	0	0	0	0
A2	Amphipathic helix	0	0.75	0.25	0	0
B1	Half-bilayer	0	0.36	0.64	0	0
C1	Full bilayer, even	0	0.18	0.32	0.32	0.18
C2	Full bilayer, 2:1	0	0.24	0.43	0.21	0.12
C3	Full bilayer, 1:2	0	0.12	0.21	0.43	0.24
D	Molecular construction	0.09	0.19	0.35	0.37	0

*Regions defined in Fig. 3.

cytochrome b_5, is that of an amphipathic helix lying in the plane of the membrane (Segrest and Jackson, 1977). Incorporation of a protein in this manner effectively increases the surface area of the bilayer, thereby decreasing its thickness; this effect has been taken into account by reducing the model bilayer thickness by two density strips (4 Å), removed from the center of the profile calculated for this model (A2). A simple modification of the bilayer-spanning model (and one that tests the level of discrimination possible with this approach) is an uneven distribution of the protein volume between the two lipid monolayers. Models C2 and C3 represent a partitioning of the cytochrome b_5 hydrophobic peptide in the mass ratio of 2:1 between the halves of the bilayer, with an even distribution within each half of the bilayer. Finally, a molecular model of cytochrome b_5, derived from previously discussed considerations (Dailey and Strittmatter, 1981), has been compared with the general models described above. Its mass distribution in profile is listed as model D in Table II.

Structure factors and phase relationships derived from model profiles were tested by calculating a residual against the information contained in the data. Although phases are not determined by contrast variation, the phase of each structure factor is defined relative to that at another D_2O content. Because data sets in three different H_2O-D_2O mixtures are required for this determination, their information content is nondegenerate, and all should be included in a test of models. A residual that takes all data points and phase information into account is defined by

$$R = \frac{\sum_h \sum_X |\epsilon_{ass}(h, X) \cdot F_{obs}(h, X) - K^X \cdot \epsilon_{calc}(h, X) \cdot F_{calc}(h, X)|}{\sum_h \sum_X F_{obs}(h, X)} \quad (6)$$

where the summations are taken over the three H_2O-D_2O mixtures used (X = 0, 42, and 95% D_2O) and all observed diffraction orders (h = 1 to 7). Phases $\epsilon_{ass}(h, X)$ are assigned to each observed structure factor from the calculated phases $\epsilon_{calc}(h, X)$, but only insofar as consistent with the observed phase variation. Observed and calculated structure factors are scaled by a factor K that sets equal the sums (over h and X) of their squares. The residuals calculated for the various model profiles are listed in Table III.

The significance of differences between residuals is difficult to measure objectively. A statistical basis for comparison of models to diffraction data has been suggested by Hamilton (1964), and involves the formulation of a weighted residual, which for this case has been calculated as

$$R' = \left\{ \frac{\sum_X \sum_h w(h, X)[\epsilon_{ass}(h, X) F_{obs}(h, x) - K\epsilon_{calc}(h, X) F_{calc}(h, X)]^2}{\sum_X \sum_h w(h, X) [F_{obs}(h,X)]^2} \right\}^{1/2} \quad (7)$$

where the weights $w(h, X)$ are the inverse variances of the observed structure factors, and the other quantities are defined for Eq. 6. Models can be compared individually with the model giving the lowest residual value, and, taking into account the number of data points and parameters varied between models, confidence levels for rejection can be derived from probability tables. Quantitation of the operational differences between models is not straightforward, but a reasonable approach is to compare the number of ways in which each model differs from the most favored one. The distribution of the cytochrome b_5 hydrophobic segment can differ from that of model C3 in the ratio between the halves of the bilayer, within each half of the bilayer, and between the bilayer and the aqueous space. Other variable parameters are optimized for each model, and are not differences between models. By this criterion,

TABLE III
RESIDUALS CALCULATED BETWEEN MODELS AND DATA

Model*	R‡	Head + link§	R'‖	Confidence level¶
		Å		
A1	0.600	28	0.142	0.95
A2	0.601	34	0.182	0.99
B1	0.527	36	0.128	0.90
C1	0.447	32	0.121	0.50
C2	0.471	32	0.123	0.75
C3	0.420	32	0.120	—
D	0.455	32	0.122	0.50

*Models defined in Table II.
‡Defined by Eq. 6.
§Profile projection of the extramembranous part of the cytochrome b_5 structure.
‖Defined by Eq. 7.
¶Approximate statistical confidence level for rejection of a model in favor of the best model, based on R' value and number of parameters and data points (see Discussion).

models A1, B1, C1, and C2 differ from C3 by only one parameter, while model A2 differs by two, and model D by all four. Estimates of confidence levels for rejection of these models, based on this assessment of parameters and using all 21 independent data points, are listed in Table III. The results of this evaluation support the conclusions reached by calculation of the more conventional residuals. Surface-associated models and, to a lesser degree, the half-bilayer model of the cytochrome b_5 hydrophobic domain may be rejected with a reasonable level of confidence in favor of model C3. However, the various full-bilayer penetration models, as well as the previously proposed folding scheme, are in approximately equal agreement with the data. While the statistical analysis is rigorously valid only for linear analyses, which this is not, it provides some dispassionate criterion for assessing the validity of the models being considered.

DISCUSSION

The analysis described in this paper is an attempt to derive a molecular interpretation from low-resolution, one-dimensional diffraction data. Model building has been used as a method to combine previous structural knowlege of cytochrome b_5 with the information supplied by the current study. The results of this procedure indicate a preference for those models in which the cytochrome b_5 membrane-binding segment is deeply embedded in the bilayer, all favored models are optimized with a distribution of the extramembranous part of the protein localized fairly close (32 Å) to the membrane. However, discrimination among membrane-spanning models is low (compared with the other models), and the molecular construction (model D) is intermediate in the ranking of transbilayer models.

A serious question in a low-resolution, model-building analysis is whether the model is an adequate representation of the structure, and whether all relevant models have been considered. The residuals obtained for the models examined are below the value expected for a random structure, and models calculated using incorrect parameters, such as a much higher lipid-to-protein ratio, result in worse agreement with the data. As seen by the examination of the transbilayer models, fairly substantial changes in the protein distribution within the bilayer cause very small differences in the residuals. Other variations of these models, including some penetration of the bilayer into the aqueous space distal from the catalytic domain, also result in similar residuals. An exhaustive search for an optimum model may yield substantially better agreement with the data. However, by introducing more and finer parameters, the information content of the data, roughly estimated in the statistical analysis above, will surely be exceeded.

As with any reconstituted system, uncertainty concerning the structures produced must engender caution in interpretation. In the case of cytochrome b_5, numerous studies strongly support the belief that the reconstitution into vesicles is biologically relevant. However, the formation of lipid-protein multilayers is not a well-understood process. Structural changes in the lipid arrangement may be induced by protein incorporation or by multilayer formation. It is impossible to assess, and hazardous to guess, the potential effects based on the data presently reported; a reasonable assumption is that they are minor perturbations of the bilayer and do not influence the profile at low resolution. Although it is an imperfect approximation to the actual lipid organization, the derived bilayer profile has been used unaltered, except for the substitution of lipid with protein, as dictated by their respective volume fractions. Protein redistribution, causing imperfect asymmetry, is another possible result of multilayer formation. Its effect on this analysis has been explored by constructing models with a partially symmetric distribution of cytochrome b_5. Moderate degrees of symmetry (e.g., a 75:25 distribution of protein) result in slightly lower residual values for all models, with the rank order of models preserved, though with discrimination somewhat reduced. Beyond this point, the calculated structure factors for odd-numbered reflections are greatly reduced, in disagreement with the observed values. The indication from this analysis is that the cytochrome b_5 molecules are assymmetrically distributed and that modest rearrangements do not alter the conclusions we reach.

We have examined the relationship of the cytochrome b_5 molecule to the lipid bilayer using neutron diffraction data and a model building analysis. Models are favored in which the hydrophobic tail of the protein penetrates deeply into the hydrophobic region of both halves of the bilayer, possibly spanning the bilayer completely.

We wish to thank Dr. Phillip Strittmatter for providing the protein used in this work, and for advice and illuminating discussions. We are grateful to Mr. S. A. Wilson and Ms. B. A. Gillette for technical assistance, and the European Molecular Biology Organization for use of laboratory facilities for some of the sample preparation.

This work was supported by National Institutes of Health grants GM29243 and GM22778 and National Science Foundation grant PCM 78-10361.

Received for publication 10 August 1982.

REFERENCES

Bartlett, G. R. 1959. Phosphorous assay in column chromatography. *J. Biol. Chem.* 234:466.

Blaurock, A. E. 1975. Bacteriorhodopsin: a transmembrane pump containing α-helix. *J. Mol. Biol.* 93:139.

Bligh, E. G., and W. J. Dyer. 1959. Extraction of bacterial lipids. *Can. J. Biochem. Physiol.* 37:911.

Buldt, G., H. U. Gally, J. Seelig, and G. Zaccai. 1979. Neutron diffraction studies on phosphatidylcholine model membranes. I. Head group conformations. *J. Mol. Biol.* 134:673.

Caspar, D. L. D., and W. C. Phillips. 1975. Dynamical effects in small-angle neutron diffraction from membranes. *Brookhaven Symp. Biol.* 27:(VII) 107–125.

Chapman, D., and A. Morrison. 1966. Physical studies of phospholipids. IV. High resolution nuclear magnetic resonance spectra of phospholipids and related substances. *J. Biol. Chem.* 241:5044.

Dailey, H. A., and P. Strittmatter. 1981. Orientation of the carboxy and

NH_2 termini of the membrane-binding segment of cytochrome b_5 on the same side of phospholipid bilayers. *J. Biol. Chem.* 256:3951.

Dupont, Y., S. C. Harrison, and W. Hasselbach. 1973. Molecular organization in the sarcoplasmic reticulum membrane studied by x-ray diffraction. *Nature (Lond.)*. 244:555.

Enoch, H. G., P. J. Fleming, and P. Strittmatter. 1979. The binding of cytochrome b_5 to phospholipid vesicles and biological membranes. *J. Biol. Chem.* 254:6438.

Fleming, P. J., H. A. Dailey, D. Corcoran, and P. Strittmatter. 1978. The primary structure of the nonpolar segment of bovine cytochrome b_5. *J. Biol. Chem.* 253:5369.

Fleming, P. J., D. E. Koppel, A. L. Y. Lau, and P. Strittmatter. 1979. Intramembrane position of the fluorescent tryptophanyl residue in membrane-bound cytochrome b_5. *Biochemistry.* 18:5458.

Franks, N. P., and W. R. Lieb. 1979. The structure of lipid bilayers and the effects of general anaesthetics. *J. Mol. Biol.* 133:469.

Hamilton, W. C. 1964. Statistics in the Physical Sciences. Ronald Press, NY.

Hagihara, B., N. Sato, and T. Yamanaka. 1975. Type *b* cytochromes. *The Enzymes.* 11:549.

Herbette, L., A. Scarpa, J. K. Blaisie, C. T. Wang, A. Saito, and S. Fleischer. 1981. Comparison of the profile structures of isolated and reconstituted sarcoplasmic reticulum membranes. *Biophys. J.* 36:47–72.

Huang, C. 1969. Studies on phosphatidylcholine vesicles. Formation and physical characteristics. *Biochemistry.* 8:344.

Jacrot, B. 1976. The study of biological structures by neutron scattering from solution. *Rep. Progr. Phys.* 39:911.

Kajihara, T., and B. Hagihara. 1968. Preparation of crystalline cytochrome b_5 from rabbit liver. *J. Biochem. (Tokyo).* 63:453.

Kirschner, D. A., D. L. D. Caspar, B. P. Schoenborn, and A. C. Nunes. 1975. Neutron diffraction studies of nerve myelin. *Brookhaven Symp. Biol.* 27:(III) 68–76.

Levine, Y. K., and M.H. F. Wilkins. 1971. Structure of oriented lipid bilayers. *Nat. New Biol.* 230:69.

Mathews, F. S., P. Argos, and M. Levine. 1971. The structure of cytochrome b_5 at 2:0 Å resolution. *Cold Spring Harbor Symp. Quant. Biol.* 36:387.

Moore, P. B., D. M. Engelman, and B. P. Schoenborn. 1975. A neutron scattering study of the distribution of protein and RNA in the 30 S ribosomal subunit of *Escherichia coli. J. Mol. Biol.* 91:101.

Morrison, W. R., and L. M. Smith. 1964. Preparation of fatty acid methyl esters and dimethylacetals from lipids with boron fluoride-methanol. *J. Lipid Res.* 5:600.

Ozols, J., and P. Strittmatter. 1969. Correction of the amino acid sequence of calf liver microsomal cytochrome b_5. *J. Biol. Chem.* 244:6617.

Rogers, M. J., and P. Strittmatter. 1975. The interaction of NADH-cytochrome b_5 reductase and cytochrome b_5 bound to egg lecithin liposomes. *J. Biol. Chem.* 250:5713.

Saxena, A. M., and B. P. Schoenborn. 1977. Correction factors for neutron diffraction from lamellar structures. *Acta Crystallogr.* A33:813.

Schoenborn, B. P. 1976. Neutron scattering for the analysis of membranes. *Biochim. Biophys. Acta.* 457:41.

Segrest, J. P., and R. L. Jackson. 1977. Molecular properties of membrane proteins. *In* Membrane Proteins and their Interactions with Lipids. R. A. Capaldi, editor. Marcel Dekker, Inc., New York.

Spatz, L., and P. Strittmatter, 1971. A form of cytochrome b_5 that contains an additional hydrophobic sequence of 40 amino acid residues. *Proc. Natl. Acad. Sci. USA.* 68:1042.

Stockton, G. W., C. F. Polnaszek, L. C. Leitch, A. P. Tulloch, and I. Smith. 1974. A study of mobility and order in model membranes using ^2H NMR relaxation rates and quadrupole splittings of specifically deuterated lipids. *Biochem. Biophys. Res. Commun.* 60:844.

Strittmatter, P., P. J. Fleming, M. Connors, and D. Corcoran. 1978. Purification of cytochrome b_5. *Methods Enzymol.* 52:97.

Tardieu, A., V. Luzzati, and F. C. Reman. 1973. Structure and polymorphism of the hydrocarbon chains of lipids: a study of lecithin-water phases. *J. Mol. Biol.* 75:711.

Visser, L., N. C. Robinson, and C. Tanford. 1975. The two-domain structure of cytochrome b_5 in deoxycholate solution. *Biochemistry.* 14:1194.

von Jagow, G., and W. Sebald. 1980. *b*-Type cytochromes. *Annu. Rev. Biochem.* 49:281.

Wilkins, M. H. F., A. E. Blaurock, and D. M. Engelman. 1971. Bilayer structure in membranes. *Nat. New Biol.* 230:72.

Worcester, D. L. 1975. Neutron beam studies of biological membranes and membrane components. *In* Biological Membranes 3:1. D. Chapman and D. F. H. Wallach, editors. Academic Press Inc. Ltd., London.

Worcester, D. L., and N. P. Franks. 1976. Structural analysis of hydrated egg lecithin and cholesterol bilayers. II. Neutron diffraction. *J. Mol. Biol.* 100:359.

Worthington, C. R. 1969. The interpretation of low-angle x-ray data from planar and concentric multilayered structures. *Biophys. J.* 9:222.

Yeager, M. J., B. Schoenborn, D. Engelman, P. Moore, and L. Stryer. 1980. Neutron diffraction analysis of the structure of rod photoreceptor membranes in intact retinas. *J. Mol. Biol.* 137:315.

Zaccai, G. 1978. Application of neutron diffraction to biological problems. *Top. Curr. Phys.* 6:243.

Zaccai, G., J. K. Blaisie, and B. P. Schoenborn. 1975. Neutron diffraction studies on the location of water in lecithin bilayer model membranes. *Proc. Natl. Acad. Sci. USA.* 72:376.